Molecular Pharmacology Fast Forward. Published on November 8, 2007 as doi:10.1124/mol.107.039024
This article has not been copyedited and formatted. The final version may differ from this version.

BubR1 is required for a sustained mitotic spindle checkpoint arrest in human cancer cells treated with tubulin targeting pyrrolo-1,5-benzoxazepines.

Lisa M. Greene, Giuseppe Campiani, Mark Lawler, D. Clive Williams, and Daniela M Zisterer.

School of Biochemistry and Immunology, Trinity College, Dublin 2, Ireland (L.M.G., D.C.W., D.Z.); Dipartimento Farmaco Chimico Tecnologico, Universita'degli Studi di Siena, Italy (G.C.); Institute of Molecular Medicine, St. James's Hospital and Trinity College, Dublin 2, Ireland (M.L.).

Molecular Pharmacology Fast Forward. Published on November 8, 2007 as DOI: 10.1124/mol.107.039024
This article has not been copyedited and formatted. The final version may differ from this version.

Running title: BubR1 is essential for PBOX-induced G_2M arrest

Correspondence to: Dr. Lisa Greene, School of Biochemistry and Immunology, Trinity College, Dublin 2, Ireland. E-mail: greeneli@tcd.ie; Tel: 00 353 1 8961855; Fax: 00 353 1 6772400.

Pages: 37

Figures: 8

References: 33

Words in Abstract: 205

Words in Introduction: 729

Words in Discussion: 1127

Abbreviations: PBOX, pyrrolo-1,5-benzoxazepine; PBS, phosphate buffered saline; SDS, sodium dodecyl sulphate; PAGE, polyacrylamide gel electrophoresis; TBS-T, Tris buffered saline pH 7.6/0.05% Tween-20; HRP, horse radish peroxidase; FCS, foetal calf serum; PI, propidium iodide; JNK, c-Jun NH_2-terminal kinase; MTA, microtubule targeting agent; CML, chronic myeloid leukemia; Ph, Philadelphia chromosome; mAb, monoclonal antibody; ECL, enhanced chemiluminescence; PVDF, polyvinylidene difluoride; SEM, standard error of the mean; APC/C, anaphase promoting complex/cyclosome; DMSO, Dimethyl Sulfoxide; DTT, dithiothreitol; RT, room temperature; RNA, Ribonucleic acid; DNA, Deoxyribonucleic acid; FACS, Fluorescence Activated Cell Sorting; DMEM, Dulbecco's Modified Eagle's Medium.

Molecular Pharmacology Fast Forward. Published on November 8, 2007 as DOI: 10.1124/mol.107.039024
This article has not been copyedited and formatted. The final version may differ from this version.

Abstract

Intrinsic or acquired resistance to chemotherapy is a major clinical problem which has evoked the need to develop innovative approaches to predict and ultimately reverse drug resistance. A prolonged G_2M arrest has been associated with apoptotic resistance to various microtubule targeting agents (MTAs). In this study, we describe the functional significance of the mitotic spindle checkpoint proteins; BubR1 and Bub3, in maintaining a mitotic arrest following microtubule disruption by nocodazole and a novel series of MTAs, the pyrrolo-1,5-benzoxazepines (PBOXs) in human cancer cells. Cells expressing high levels of BubR1 and Bub3 (K562, MDA-MB-231 and Hela) display a prolonged G_2M arrest following exposure to MTAs. On the other hand, cells with low endogenous levels of mitotic spindle checkpoint proteins (SK-BR-3 and HL-60) transiently arrest in mitosis and undergo increased apoptosis. The phosphorylation of BubR1 correlated with PBOX-induced G_2M arrest in four cell lines tested indicating an active mitotic spindle checkpoint. Gene silencing of BubR1 by siRNA interference reduced PBOX-induced G_2M arrest without enhancing apoptotic efficacy. Further analysis demonstrated that PBOX treated BubR1-depleted cells were both mononucleated and multinucleated with a polyploid DNA content suggesting a requirement for BubR1 in cytokinesis. Taken together, these results suggest that BubR1 contributes to the mitotic checkpoint induced by the PBOXs.

Molecular Pharmacology Fast Forward. Published on November 8, 2007 as DOI: 10.1124/mol.107.039024
This article has not been copyedited and formatted. The final version may differ from this version.

Microtubules are dynamic polymers that play a fundamental role in a number of cellular functions ranging from cell division to cell motility (Mollinedo and Gajate, 2003). Hence, microtubule targeting agents (MTAs) represent some of the most clinically successful chemotherapeutic drugs identified to date. Tubulin is the principle component of microtubules. MTAs function by affecting the equilibrium between free tubulin dimers and assembled polymers. Collectively, MTAs comprise of a diverse group of anti-mitotic drugs which may be subdivided into two distinct categories; those that inhibit microtubule polymerisation e.g. vinca alkaloids and nocodazole, and those that promote microtubule polymerisation and subsequent stabilisation of the microtubules e.g. paclitaxel (Jordan, 2002). The clinical success of the taxanes and vinca alkaloids has evoked a major search for new drugs that perturb mitotic spindle microtubule dynamics and function.

We recently described a novel group of tubulin targeting compounds namely; the pyrrolo-1,5-benzoxazepines (PBOXs), which are structurally distinct from the aforementioned MTAs (Mulligan *et al.* 2006). PBOX-6, a representative member of the PBOX compounds, functions by inhibiting microtubule polymerisation followed by cell cycle arrest at G_2M and late apoptosis (Mulligan *et al*., 2006). PBOX-6 induced many of the biochemical hallmarks of apoptosis including PARP cleavage, cytoplasmic blebbing, DNA fragmentation and positive-tunnel staining (Greene *et al*., 2005; Mc Gee *et al*., 2002a). A cell type specific dependence of caspases on PBOX-6-induced apoptosis was observed (Mc Gee *et al*., 2002a; Zisterer *et al*., 2000), a trait shared with paclitaxel (Ofir *et al*., 2002). As demonstrated with other MTAs, we have shown that activation of JNK,

Molecular Pharmacology Fast Forward. Published on November 8, 2007 as DOI: 10.1124/mol.107.039024
This article has not been copyedited and formatted. The final version may differ from this version.

together with the phosphorylation and inactivation of the anti-apoptotic proteins Bcl-2 and Bcl-x_L are a prerequisite for PBOX-6-induced apoptosis (Mc Gee *et al*., 2002b; Mc Gee *et al*., 2004). PBOX-6 induced apoptosis in a wide spectrum of cancer cells without displaying any activity towards normal blood cells (Zisterer *et al*., 2000; Mc Gee *et al*., 2001; Mc Gee *et al.*, 2004; Greene *et al*., 2005). Interestingly, unlike the taxanes, PBOX-6-induced apoptosis is independent of Bcl-2 and Her-2 expression levels (Mc Gee *et al.* 2004; Greene *et al*., 2005). Up-regulation of the anti-apoptotic Bcl-2 protein and the Her-2 oncogene, were previously shown to contribute to paclitaxel resistance (Tang *et al*., 1994; Yu *et al*., 1998). Furthermore, PBOX-6 displayed significant anti-tumour activity *in vivo* in an aggressive murine model of mammary carcinoma (Greene *et al*., 2005). The tumour selective effects of the tubulin-targeting PBOX compounds and apoptotic efficacy in chemotherapeutic resistant cells highlight their potential as anti-cancer agents.

It is well accepted that tubulin-targeting agents principally function by disrupting microtubule dynamics during mitosis and subsequent activation of the mitotic spindle checkpoint leading to mitotic cell cycle arrest. Exposure to MTAs can induce differential responses in different cell types. Some cells exhibit a sustained mitotic arrest whilst others only arrest transiently in mitosis and proceed to undergo apoptosis. The mitotic spindle checkpoint monitors both the attachment of chromosomes to the mitotic spindle and the tension across the sister chromatids generated by microtubules. The checkpoint signal is generated at the kinetochore, a large multiprotein subunit that is located on the centromere of each chromosome and mediates the attachment of chromosomes to the mitotic spindle (Cleveland *et al*., 2003). There is substantial evidence to suggest that the

checkpoint prevents cell cycle progression by inhibiting the activity of the anaphase promoting complex/cyclosome (APC/C) (Acquaviva *et al*., 2004). The APC/C, is an ubiquitin ligase which upon interaction with its co-activator, Cdc-20, targets anaphase inhibitors (securin/Pds1) and mitotic cyclins (cyclin B) for proteasome mediated degradation (Peters, 2002). This cascade of events ultimately leads to cohesion degradation and chromosomal separation (Peters, 2002; Doncic *et al*., 2005). Several key mitotic spindle checkpoint proteins (Bub1, BubR1, Mps1, Bub3, Mad1-3) have been identified which bind to Cdc-20 and prevent activation of the APC/C and in doing so inhibit anaphase progression. Interestingly, a recent study conducted by Logarinho *et al*., (2004) suggested that spindle checkpoint proteins sense distinct aspects of kinetochore interaction with the spindle, with Mad2 and Bub1 monitoring microtubule occupancy while BubR1 and Bub3 monitor tension across attached kinetochores.

In this study, we sought to determine the effects on BubR1 and Bub3 expression levels following PBOX-induced loss of microtubule tension in a panel of human cancer cells and decipher any correlation with a sustained mitotic arrest. We also characterise the anti-mitotic properties of PBOX-15, a more potent analogue of the recently described tubulin-targeting pyrrolo-1,5-benzoxazepine, PBOX-6.

Molecular Pharmacology Fast Forward. Published on November 8, 2007 as DOI: 10.1124/mol.107.039024
This article has not been copyedited and formatted. The final version may differ from this version.

Materials and Methods.

Cells. All cell lines were originally obtained from the European Collection of Cell Cultures (Salisbury, UK). The K562 cells were derived from a patient in the blast crisis stage of CML. HL-60 cells were derived from a patient with acute myeloid leukaemia. MDA-MB-231 and SK-BR-3 cells originate from a peural effusion from patients with metastatic adenocarcinoma of the breast. Hela cells are cervical adenocarcinoma-derived. K562 cells and HL-60 cells were cultured in RPMI-1640 medium. MDA-MB-231 and Hela cells were grown in Dulbecco's Modified Eagle's Medium (DMEM). SK-BR-3 cells were grown in McCoy's 5a Medium Modified. HL-60 cells were maintained in medium enhanced with 20% FCS and all other cell lines were grown in media supplemented with 10% FCS. All media was supplemented with 100 units/ml penicillin, 100 μg/ml streptomycin and 2 mM glutamine. Cells were maintained at 37°C in 5% CO_2 in a humidified incubator.

Reagents. PBOX-6 (7-[(dimethylcarbamoyl) oxy]-6-(2-naphthyl)pyrrolo-[2,1-*d*][1,5][benzoxazepine) and -15 (4-acetoxy-5-(-1-(naphthyl)naphtho[2,3-*b*]pyrrolo[2,1-*d*] [1,4]oxazepine) were synthesised as described previously (Campiani *et al*., 1996), and dissolved in ethanol. Structures of the PBOX compounds were described by Mulligan *et al*., (2006). Nocodazole was purchased from Sigma Chemical Co. (Poole, Dorset, UK), and dissolved in sterile DMSO. All compounds once dissolved in the relevant solvent were stored at –20^{o}C. Cell culture medium was purchased from Gibco, Invitrogen Corp. (Grand Island, NY, USA). L-glutamine and penicillin/streptomycin were supplied from

Molecular Pharmacology Fast Forward. Published on November 8, 2007 as DOI: 10.1124/mol.107.039024
This article has not been copyedited and formatted. The final version may differ from this version.

Sigma. The anti-Bub3 mouse monoclonal antibody (mAb) and the mouse anti-BubR1 mAb were purchased from BD Transduction Laboratories (Cowley, UK). The anti-actin mAb and anti-tubulin antibodies were obtained from Merck Biosciences (Nottingham, UK). FITC anti-mouse and Cy3 anti-sheep antibodies were purchased from Jackson Immunoresearch (Suffolk, UK). The enhanced chemiluminescence (ECL) reagent was obtained from Amersham Biosciences (Buckinghamshire, UK). For siRNA experiments, the siRNA duplexes were supplied from Ambion (Huntingdon, UK) and the oligofectamine transfection reagent was purchased from Invitrogen (Paisley, UK). All other chemicals were obtained from Sigma.

Western blot analysis. After treatment, whole cell pellets were washed in PBS, resuspended in 60 µl of PBS, lysed by the addition of 60 µl 2X Laemmli buffer [1X = 30 mM Tris-base (pH 6.8), 2% SDS, and 10% glycerol] and briefly sonicated. Homogenates were quantified by the Markwell protein assay prior to addition of reducing agent (50 mM DTT). Samples were boiled for 3 min and equal amounts of protein were separated by SDS-PAGE, and electroblotted to PVDF membrane. The blots were stained in 0.1% Ponceau S (w/v) in 5% acetic acid (v/v) to ensure equal transfer. Membranes were briefly washed in Tris-Buffered Saline, pH 7.6; 0.05% Tween-20 (TBS-T) and blocked for at room temperature (RT) in TBS-T containing 5% (w/v) dried milk (blocking buffer). After 1 h, the blots were then incubated overnight at 4^{o}C in 1 µg/ml primary antibody diluted in 5% blocking solution. Blots were then washed 3 x 10 min in TBS-T and incubated for 1 h at RT in a 1:1000 dilution of horseradish peroxidase-conjugated secondary antibody.

Molecular Pharmacology Fast Forward. Published on November 8, 2007 as DOI: 10.1124/mol.107.039024
This article has not been copyedited and formatted. The final version may differ from this version.

Blots were again washed 3 x 10 min in TBS-T and developed by enhanced chemiluminescence.

Drug Treatment. For the suspension cells, logarithmically growing cells were seeded at 200,000/ml (K562) 300,000/ml (HL-60) in sterile plastic T-flasks. For adherent cells, cells were seeded at a density of 3.4 x 10^4/cm^2 (SK-BR-3), 4 x 10^4/cm^2 (MDA-MB-231) and 9.2 x 10^3/cm^2 (Hela) for 24 h prior to drug treatment. Cells were left untreated, or treated with solvent control, or with the designated concentration of drug for the specified period of time. At the end of the incubation period, cells were harvested by centrifugation at 600 x *g* for 10 min at room temperature, and prepared for subsequent analysis as detailed below.

Determination of DNA content. The flow cytometric evaluation of cellular DNA content was performed as previously described (Greene *et al*., 2005). Briefly, after treatment of adherent cell lines, floating cells were collected and then pooled with attached cells removed by trypsinisation. Once collected, all cell types were then centrifuged at 800 x *g* for 10 min and resuspended in ice cold PBS (200 µl). Cells were then fixed by a dropwise addition of 70% ethanol:PBS (2 ml) while gently vortexing the cells. Following fixation for at least 1 h at -20^{o}C and addition of 0.25% FCS, cells were again centrifuged and resuspended in PBS containing 10 µg/ml RNase A and 100 µg/ml propidium iodide (PI). Cells were then incubated for 30 min in the dark at 37^{o}C. The PI fluorescence was measured on a linear scale using a FACSCalibur flow cytometer (Becton Dickinson, San Jose, CA). The amount of PI fluorescence is directly proportional

Molecular Pharmacology Fast Forward. Published on November 8, 2007 as DOI: 10.1124/mol.107.039024
This article has not been copyedited and formatted. The final version may differ from this version.

to the amount of DNA present in each cell. The relative content of DNA indicates the distribution of a population of cells throughout the cell cycle. For example, cells in G_0G_1 are diploid and have a DNA content of 2N. Cells with the G_2M phases have a DNA content of 4N, while cells in S-phase have a DNA content between 2N and 4N. Apoptotic cells are sub-diploid (<2N) and polyploid cells have a >4N DNA content. Data collection was gated to exclude cell debris and cell aggregates. At least 10,000 cells were analysed per sample. All data were recorded and analysed using the CellQuest software (Becton Dickinson).

Small-interfering RNA (siRNA) transfection. In this study, we used a validated siRNA duplex to target the BubR1 sequence 5'-GGUGGGAAGGAGAGUAAUATT-3' (Ambion, UK). A scrambled RNA duplex was used as a control (5'-AGGGUAGUAGGAGAUGATT-3'). The selected siRNAs were BLAST searched against the human genome sequence to ensure only one gene was targeted, whereas the control scrambled siRNA sequence used has no known overlap. Cells were seeded at density of 7.2 x $10^3/cm^2$ (Hela) and 1.8 x$10^4/cm^2$ (MDA-MB-231) in DMEM without antibiotics. After 24 h, the transfection was carried out on 50% confluent cells in Optimen medium using oligofectamine transfection reagent (Invitrogen, CA) in accordance with the manufacturer's instructions. The siRNA complexes were removed after 4 or 24 h and replaced with DMEM supplemented with 20% FCS. Cells were analysed 24-120 hours post-transfection.

Molecular Pharmacology Fast Forward. Published on November 8, 2007 as DOI: 10.1124/mol.107.039024
This article has not been copyedited and formatted. The final version may differ from this version.

Immunofluorescence and confocal microscopy. For immunofluorescence, Hela cells were grown on poly-L-lysine-coated coverslips. Following treatment cells were washed twice with PBS, washed once with microtubule stabilizing buffer (100 mM PIPES pH 6.8, 1 mM MgCl, 0.1 mM $CaCl_2$, 0.1% Triton X-100) at room temperature, then fixed for 10 min in 4% formaldehyde diluted in the microtubule stabilizing buffer. Following washes in PBST (PBS and 0.1% Triton-X-100), cells were blocked in 5% non-fat dried milk (Marvel) diluted in PBST (blocking buffer). Cells were then incubated with primary antibodies mouse anti-tubulin (DM1A; 1:20) and sheep anti-BubR1 (SBR1.1; 1:1000) (kindly provided by Dr. Stephen Taylor, School of Biological Sciences, University of Manchester) for 1 h at room temperature. Following washes in PBST cells were incubated with secondary antibodies (FITC anti-mouse and Cy3 anti-sheep) for 1 h at room temperature. Following washes in PBST, the cells were stained with Hoechst 33258 at 1 μg/ml in PBS for 5 minutes, mounted in 4 % propyllgallate in PBS:glycerol. Projected images from a z-series of 15-22 stacks of confocal images acquired at 0.6 μM intervals were captured using the OLYMPUS 1X81 microscope coupled with OLYMPUS FLUOVIEW Ver 1.5 software. All images in each experiment were collected on the same day using identical parameters.

Statistical Analysis. The statistical analysis of experimental data was performed using a Student's paired *t*-test and results were presented as mean ± S.E.M. A value of $P \leq 0.05$ was considered to be significant.

Molecular Pharmacology Fast Forward. Published on November 8, 2007 as DOI: 10.1124/mol.107.039024
This article has not been copyedited and formatted. The final version may differ from this version.

Results

Effects of PBOX-15, a novel pyrrolo-1,5-benzoxazepine, on the cell cycle and apoptosis in K562 cells. We have previously reported that PBOX-6, a representative member of the pro-apoptotic subset of PBOX compounds, induced apoptosis in K562 cells following a prolonged G_2M cell cycle arrest (Mulligan *et al*., 2006). In this manuscript, we describe a novel more potent anti-mitotic member of the PBOX series, PBOX-15. PBOX-15 (IC50; 0.2 μM) is 11-fold more effective at inducing a G_2M cell arrest in K562 cells than PBOX-6 (IC50; 2.2 μM) (Figure 1A). As observed in the present study and previously with PBOX-6 (Mulligan *et al*., 2006), PBOX-15-induced G_2M cell cycle arrest is detected as early as 2 h, peaks at 16 h, is sustained up to 24 h and finally begins to decline at 48 h (Figure 1B). Again, as previously shown with PBOX-6, the prolonged G_2M cell cycle arrest induced by PBOX-15 is followed by late apoptosis at 48 h (Figure 1C).

Phosphorylation of the mitotic spindle checkpoint protein BubR1 is associated with a sustained G_2M cell cycle arrest following treatment with tubulin-targeting PBOX compounds in K562 cells. As already discussed, PBOX-induced apoptosis in K562 cells is a delayed event following a prolonged G_2M cell cycle arrest. In this study, western blot analysis was used to determine whether the mitotic spindle checkpoint proteins BubR1 and Bub3 are associated with PBOX-induced G_2M cell cycle arrest. Both proteins have been shown to monitor tension across attached kinetochores and initiate mitotic arrest in response to loss of microtubule tension. As shown in Figure 2, a slower migrating form of BubR1 was predominately found in cells treated with higher doses of PBOX-6 [≥ 5

Molecular Pharmacology Fast Forward. Published on November 8, 2007 as DOI: 10.1124/mol.107.039024
This article has not been copyedited and formatted. The final version may differ from this version.

μM] and -15 [≥ 0.25 μM] which caused microtubule disruption as indicated by a significant increase in the percentage of cells arrested in the G_2M phase of the cell cycle (Figure 1). It is well documented that this slower migrating form of BubR1 represents a hyperphosphorylated form of BubR1 (Li *et al*., 1999; Chan *et al*., 1999). Furthermore, hyperphosphorylated BubR1 has been related to an active mitotic checkpoint in nocodazole blocked mitotic cells (Chan *et al*., 1999). Nocodazole treated K562 cells where included as a positive control for BubR1 hyperphosphorylation (Figure 2B). Unlike BubR1, the levels of Bub3 protein remained unchanged in G_2M arrested K562 cells treated with PBOX-6, -15 or nocodazole for 16 h (Figure 2A, B). Given that PBOX-15 is a more potent activator of the mitotic spindle checkpoint as compared to PBOX-6, we next analysed the effect of PBOX-15 [1 μM] on BubR1 phosphorylation over time. Again, cells treated with nocodazole [0.5 μM] a known stimulator of BubR1 phosphorylation was used a positive control. The hyperphosphorylated form of BubR1 was most prominent at 16 and 24 h following PBOX-15 and nocodazole treatment (Figure 2C). At this time the maximum G_2M cell cycle block was observed with 75% of PBOX-15 treated cells in the G_2M phase (Figure 1B). Interestingly, the BubR1 protein is undetectable at 48 h post PBOX-15 treatment in K562 cells (Figure 2C). At this time, a significant decline in the percentage of G_2M arrested cells was observed with a corresponding increase in the percentage of apoptotic cells (Figure 1B, C).

Inducibility of mitotic checking in response to MTAs correlates with endogenous levels of the mitotic spindle checkpoint proteins BubR1 and Bub3 in human cancer cells. To further investigate the association of BubR1 and Bub3 with MTA-induced G_2M

Molecular Pharmacology Fast Forward. Published on November 8, 2007 as DOI: 10.1124/mol.107.039024
This article has not been copyedited and formatted. The final version may differ from this version.

cell cycle arrest and apoptosis, we analysed the absolute levels of both proteins and drug sensitivity to three MTAs (PBOX-6, -15 and nocodazole) in five human cancer cell lines of different neoplastic origin. One cervical carcinoma cell line (Hela), two leukemia (K562 and HL-60) and two breast carcinoma (SK-BR-3 and MDA-MB-231) cell lines were tested. Effects of MTA treatment on BubR1 phosphorylation was also assessed in cells expressing detectable levels of BubR1. As shown in Figure 3A, levels of the mitotic spindle checkpoint regulators BubR1 and Bub3 are dysregulated in human cancers. Levels of BubR1 and Bub3 were high in K562, Hela and MDA-MB-231 cells and low to undetectable in HL-60 and SK-BR-3 cells. We next examined the susceptibility of these cell lines to MTA (PBOX-6,-15 and nocodazole)-induced G_2M cell cycle arrest and apoptosis to decipher any correlation with the mitotic spindle checkpoint. The extent of G_2M cell cycle arrest in response to depolymerisation on the microtubules was highest in spindle checkpoint-proficient cells (K562 (Figure 1), Hela and MDA-MB-231 (Figure 3B)) and lowest in spindle checkpoint-deficient cells (SK-BR-3 and HL-60) (Figure 3B). Accordingly, the levels of MTA-induced apoptosis were inversely related to the levels of mitotic spindle checkpoint proteins in these cell lines. Specifically, in cells expressing high levels of BubR1 and Bub3 up to 75% of cells were arrested in the G_2M phase after a 24 h treatment with PBOX-6, -15 or nocodazole. In direct contrast, in SK-BR-3 cells which express low levels of both BubR1 and Bub3, $\leq$35% cells were in the G_2M phase at 24 h, with levels decreasing dramatically to <3% at 48 h post MTA treatment. Furthermore, after 24 h there was no notable increase in the percentage of cells in the G_2M phase of HL-60 cells treated with MTAs as compared to control treated cells. A more detailed analysis of the effect of PBOX-6 and -15 on the cell cycle of HL-60 cells

Molecular Pharmacology Fast Forward. Published on November 8, 2007 as DOI: 10.1124/mol.107.039024
This article has not been copyedited and formatted. The final version may differ from this version.

demonstrated a transient G_2M arrest commencing at 2 h and peaking at 8 h (supplemental data; Figure 3.1). A sustained G_2M arrest was not observed in these cells following MTA exposure, a finding consistent with the low levels of mitotic spindle checkpoint proteins found in HL-60 cells. In addition, after a 48 h exposure to MTAs the maximum levels of apoptosis (>60%) were observed in spindle checkpoint compromised SK-BR-3 and HL-60 cells (Figure 3B). Apoptosis was determined by quantification of the pre-G1 peak. In contrast, significantly lower levels of apoptosis (≤ 37%) were observed in the spindle checkpoint proficient cells (K562 (Figure 1), MDA-MB-231 and Hela (Figure 3B)). This observed reduction in the percentage of apoptotic cells was accompanied by an increase in the percentage of cells remaining in the G_2M phase of the cell cycle. Apoptosis is characterised, at least in part, by the cleavage of PARP (116 kDa) into 89- and 24-kDa fragments that contain the active site and the DNA-binding domain of the enzyme, respectively. In this study, the onset on apoptosis correlated with PARP cleavage (Figure 4A). Collectively, these findings suggest that a functional mitotic spindle checkpoint may contribute to a sustained G_2M cell cycle arrest following microtubule disruption induced by tubulin-targeting pyrrolo-1,5-benzoxazepines and the tubulin depolymeriser, nocodazole.

We next examined the effects of PBOX and nocodazole exposure on BubR1 phosphorylation in cells expressing detectable levels of BubR1. Of the 5 cell lines tested in this study, MDA-MB-231 cells displayed the highest level of resistance to MTA (PBOX-6,-15 and nocodazole) exposure with an average of 55% of cells remaining in the G_2M phase after 48 h. Interestingly, levels of the phosphorylated form of BubR1

remained high in these cells at 48 h post MTA treatment suggestive of an active spindle checkpoint (Figure 4B). In Hela cells, the decline in the percentage of G_2M arrested cells from approximately 56% at 24 h to 25% at 48 h post MTA exposure coincided with a significant decrease in BubR1 protein levels. In SK-BR-3 cells, BubR1 phosphorylation was again associated with MTA-induced G_2M arrest at 24 h. Furthermore, the decline in the percentage of G_2M arrested SK-BR-3 cells at 48 h post MTA treatment was once more associated with a reduction in BubR1 protein levels. It is worth noting that in contrast to K562 (Figure 2), MDA-MB-231 and Hela cells (Figure 4B), phosphorylation of BubR1 was not detected in SK-BR-3 cells treated with PBOX-6 for 24 h (Figure 4B). However, at 24 h PBOX-6 did not induce a G_2M cell cycle arrest in these cells (Figure 3B). In contrast, treatment with PBOX-15 and nocodazole did induce both a G_2M cell cycle arrest and phosphorylation of BubR1 in SK-BR-3 cells. Additionally, the ratio of the phosphorylated form of BubR1 to the unphosphorylated form of BubR1 was lowest in the SK-BR-3 cells as compared to K562 (Figure 2), MDA-MB-231 and Hela cells at 24 h after MTA treatment (Figure 4B). In accordance with this observation the extent of G_2M cell cycle arrest was significantly less in SK-BR-3 (Figure 3B) cells than that observed in K562 (Figure 2), MDA-MB-231 and Hela cells (Figure 3B). Taken together, these findings confirm that BubR1 is required for the activation and maintenance of the mitotic spindle checkpoint in response to MTAs.

PBOX-15 causes a complete depolymerisation of the microtubule network and alters chromosome alignment during prometaphase and metaphase. Next, we examined the effects of PBOX-15 on the morphology of the mitotic spindle and on the cellular

Molecular Pharmacology Fast Forward. Published on November 8, 2007 as DOI: 10.1124/mol.107.039024
This article has not been copyedited and formatted. The final version may differ from this version.

localization pattern of BubR1 following loss of microtubule tension induced by PBOX-15 in Hela cells. PBOX-15 can potently inhibit the assembly of tubulin *in vitro* as determined by changes in turbidity produced following the polymerization of tubulin (Mulligan *et al*., 2006). Additionally, PBOX-15 disrupted the microtubule network of the breast carcinoma cell line, MCF-7 in interphase (Mulligan *et al*., 2006). Here, using confocal imagery we demonstrate a complete depolymerisation of the microtubule network in PBOX-15-arrested prometaphase and metaphase Hela cells (Figure 5). It is well accepted that in metaphase BubR1 locates to the kinetochores during normal mitosis and mitotic arrest following mitotic insult by MTAs (Taylor *et al.*, 2001). Therefore, it may be inferred that BubR1 staining in Figure 5 depicts chromosomal location. In normal (control) prometaphase and metaphase, chromosomes are aligned and tightly organised around the metaphase plate. In PBOX-15 arrested prometaphase and metaphase cells, BubR1 staining is scattered and diffuse due to incorrect chromosome attachment/alignment owing to loss of microtubule tension.

Gene silencing of BubR1 by small interfering RNA (siRNA) leads to polyploidy following mitotic spindle disruption in Hela and MDA-MB-231 cells. To further investigate the role of BubR1 in mitotic cell cycle arrest following mitotic spindle disruption by anti-mitotic PBOX compounds and nocodazole, endogenous levels of BubR1 were reduced using RNA interference. No significant difference in BubR1 knock-down levels were observed between Hela cells exposed to the transfection complex containing BubR1 siRNA [30-100 nM] for 4 or 24 h (Figure 6A). However, increased cell viability was observed in cells exposed to the transfection complex for 4 h as

Molecular Pharmacology Fast Forward. Published on November 8, 2007 as DOI: 10.1124/mol.107.039024
This article has not been copyedited and formatted. The final version may differ from this version.

opposed to 24 h (data not shown). Hence, for all subsequent experiments cells were exposed to a transfection complex containing 50 nM siRNA duplexes for 4 h. The scrambled siRNA duplex (siRNA control) did not effect the expression levels of BubR1, verifying the specificity of the siRNA approach (Figure 6A). A time-dependent reduction in BubR1 protein levels was observed in Hela cells treated with BubR1 siRNA duplexes (Figure 6B). A maximum reduction in BubR1 expression levels was observed at 48 h post-transfection and levels remained low up to 72 h. We next used flow cytometry to determine whether suppression of BubR1 affected the cell cycle distribution of Hela cells treated with PBOX-15 and nocodazole. As anticipated, down-regulation of BubR1 reduced the percentage of cells arrested in G_2M following MTA treatment (Figure 6C). Similar results were obtained with PBOX-6 (data not shown). Depletion of BubR1 did not enhance the apoptotic efficacy of MTAs in Hela cells (Figure 6C). However, knockdown of BubR1 alone did induce up to 20% apoptosis at 3 days post-transfection in Hela cells. These results are in agreement with Kops *et al*., (2004), in which knockdown of BubR1 also caused cell death. Therefore, if the 20% cell death as a result of loss of BubR1 is accounted for, PBOX-15 and nocodazole were less effective at inducing apoptosis in BubR1 depleted cells. Additionally, PARP cleavage was somewhat reduced in BubR1-depleted Hela cells treated with MTAs as compared to BubR1 expressing Hela cells confirming our hypothesis that artificial down-regulation of BubR1 impedes the apoptotic potential of MTAs (Figure 7B). A sub-population of Hela cells appear to exhibit a senescent-like growth arrest subsequent to PBOX-15 treatment as no increase in the apoptotic peak was observed up to 4 days post PBOX-15 treatment (Figure 7A). Treatment with nocodazole produced similar results (data not shown). It is clearly evident

Molecular Pharmacology Fast Forward. Published on November 8, 2007 as DOI: 10.1124/mol.107.039024
This article has not been copyedited and formatted. The final version may differ from this version.

from the representative histograms (Figure 7A) that gene-targeting of BubR1 does not enhance the apoptotic potential of MTAs, even after 4 days. In addition, knockdown of BubR1 resulted in a significant increase in the formation of polyploidy (a cell that contains greater than two full sets of chromosomes; DNA content >4N) 48 h after microtubule disruption as compared to control cells ($P < 0.01$; Student's *t*-test; Figure 6C). These polyploid cells continued to endoreplicate overtime forming cells with 16N DNA content after 4 days (Figure 7A).

Next, given that the expression profile of Bub3 mirrored that of endogenous BubR1 in the cancer cell lines analysed in this study (Figure 3A) we sought to evaluate whether forced down-regulation of BubR1 would influence Bub3 protein levels. As depicted in Figure 7B Bub3 expression levels were not directly influenced by BubR1. Similarly, knockdown of BubR1 in Xenopus egg extracts did not affect absolute Bub3 protein levels (Chen, 2002). Jointly, these findings support the lack of involvement of BubR1 over Bub3 expression across species.

The effect of PBOX-15 on the microtubule network and morphology of BubR1-depleted cells was determined by confocal microscopy. As shown in Figure 7C, PBOX-15 depolymerised the microtubule network of Hela cells transfected with scrambled and BubR1 siRNA complexes. However, BubR1-depleted cells were giant-like in appearance and were either mono or multi-nucleated due to aberrant cycling without cytokinesis.

Molecular Pharmacology Fast Forward. Published on November 8, 2007 as DOI: 10.1124/mol.107.039024
This article has not been copyedited and formatted. The final version may differ from this version.

To further confirm the importance of BubR1 protein levels in maintaining a stable mitotic arrest and preventing polyploidy, we down-regulated BubR1 protein levels by siRNA interference in a second cell line, MDA-MB-231. The specificity of the reaction was again confirmed by western blot analysis of cells treated with BubR1 siRNA and a control scrambled sequence. As shown in Figure 8, expression of BubR1 was substantially repressed in cells treated with BubR1 siRNA duplexes as compared to control treated cells. Again, as expected, down-regulation of BubR1 resulted in a significant increase in the formation of polyploid cells following mitotic release at 48 h post PBOX-15 and nocodazole treatment ($P < 0.05$; Student's *t*-test). These findings highlight the importance of BubR1 levels in the prevention of polyploidy following mitotic spindle disruption.

Molecular Pharmacology Fast Forward. Published on November 8, 2007 as DOI: 10.1124/mol.107.039024
This article has not been copyedited and formatted. The final version may differ from this version.

Discussion

Herein we report that the mitotic spindle checkpoint regulators BubR1 and Bub3 are differentially expressed in human cancers. More importantly, the endogenous levels of the mitotic spindle checkpoint proteins directly correlated with the cellular response to microtubule disruption. The mitotic spindle checkpoint is a complex pathway conserved across species and monitors the metaphase to anaphase transition. The basic model for the spindle checkpoint defines that tension defects or unattached chromosomes activate the checkpoint delaying the onset of anaphase until such aberrations are corrected. The kinetochores attach chromosomes to the spindle. This aspect of spindle checkpoint is highly organized. The kinetochore assembly process has been carefully dissected using RNA interference coupled with quantitative optical sectioning microscopy. The checkpoint proteins Bub1, Cenp-F, BubR1, Cenp-E, Bub3 and MAD2 all transiently localise in sequence to the kinetochore (Johnson *et al*., 2004; Chen, 2002). Following accurate chromosome alignment the levels of the checkpoint proteins decline and the cell cycle continues. Failure of the kinetochore to attach the sister chromatid in alignment on the mitotic spindle will trigger a 'wait signal' and prevent anaphase onset. As mentioned, localization of the checkpoint proteins to the kinechore is an organized event and not a random process. Bub1 is required for localization of Cenp-F, BubR1, Cenp-E and MAD2 (Johnson *et al*., 2004). However, repression of either Bub1 (Johnson *et al*., 2004) or Cenp-F (Holt *et al*, 2005) did not compromise spindle checkpoint function suggesting multiple start points for the spindle checkpoint cascade. BubR1 is next in the checkpoint cascade promoting recruitment of Bub1, Bub3, Mad1, Mad2 and CENP-E (Chen, 2002).

Hence, given that the two forefront proteins, Bub1 and Cenp-F are indispensable for checkpoint function considerable interest has escalated in the next candidate, BubR1.

Gene silencing of BubR1 impairs normal spindle checkpoint function (Kops *et al*., 2004). Documentation reporting affects of BubR1 depletion on spindle checkpoint function in response to mitotic insult are conflicting. Specifically, suppression of BubR1 by siRNA interference inhibited paclitaxel-induced cell death in MCF-7 breast cancer cells (Sudo *et al*., 2004). In support of these findings, Shin *et al*., (2003) demonstrated that mutational and post-transcriptional inhibition of BubR1 reduced nocodazole-induced cytotoxicity by compromising mitotic arrest. However, in contrast to these results the apoptotic efficacy of both paclitaxel and nocodazole was increased in Hela cells following the siRNA targeted down-regulation of BubR1 (Lee *et al*., 2004). These apparent discrepancies warranted the need for additional studies in both Hela cells and other cell types to further elucidate the role played by BubR1 in MTA-induced cell death. In this study, we found that BubR1 is essential for a sustained mitotic checkpoint in response to loss of microtubule tension induced by a novel class of MTAs, the pyrrolo-1,5-benzoxazepines and the tubulin depolymeriser, nocodazole in cells of different neoplastic origin.

First, results from unmanipulated cells suggest that absolute levels of BubR1 may determine the length of stay in G_2M. In support of our hypothesis, Meraldi *et al*., (2004) demonstrated that knockdown of BubR1 accelerates the normal progression of mitosis. Furthermore, in our studies the MTA-induced G_2M block was maintained until endogenous levels of BubR1 protein became undetectable and at this point a marked

increase in apoptosis was observed. BubR1 cellular levels inversely correlated with the onset of apoptosis. These results are in agreement with recent reports suggesting that degradation of BubR1 by both a caspase-dependent (Kim *et al*., 2005) and a ubiqutin-dependent proteosome pathway (Shin *et al*., 2003) were associated with release from mitotic block following prolonged spindle damage. Collectively, these results suggest that endogenous levels of BubR1 may predict the apoptotic efficacy and potential chemotherapeutic benefit of MTAs in human cancers. In support of this hypothesis, BubR1 was found to be overexpressed in a cohort of 43 gastric carcinomas (Grabsch *et al*., 2003). Interestingly, paclitaxel failed in clinical trials in patients with gastric carcinoma (Garcia *et al*., 2001). It is possible that an overactive mitotic checkpoint may contribute to paclitaxel resistance in gastric carcinomas, amongst others.

We also report that expression levels of Bub3 mirrored that of BubR1 in the cells lines tested. This finding is interesting as both proteins are believed to evoke a spindle checkpoint in response to loss of spindle tension (Logarinho *et al*., 2004). Therefore, it was not unexpected that the weakest mitotic response to MTA-induced loss of microtubule tension was observed in the cell lines expressing the lowest levels of Bub3 and BubR1. However, mitotic insult or the onset of apoptosis did not alter the expression levels or post-translational modification, in terms of phosphorylation, of Bub3. As reported herein, and elsewhere (Meraldi *et al*., 2004) forced down-regulation of BubR1 did not influence total cellular Bub3 levels suggesting that Bub3 protein levels are not directly controlled by BubR1.

We next sought to determine whether forced down-regulation of BubR1 through the RNA interference strategy could induce a similar phenotype in terms of apoptotic susceptibility to MTAs as cells which had evolved to express low levels of BubR1. Gene silencing of BubR1 significantly reduced the accumulation of cells in the G_2M phase in cells derived from both a cervical and a breast carcinoma in response to mitotic insult. These results support previous studies demonstrating that BubR1 is essential for maintaining a mitotic arrest in response to microtubule disruption induced by the tubulin polymeriser, paclitaxel (Sudo *et al*., 2004). In our studies knockdown of BubR1 did not enhance the apoptotic efficacy of the tubulin-targeting PBOX compounds or nocodazole in human cancer cells. Depolymerisation of the microtubules and depletion of BubR1 lead to incomplete cytokinesis. Our results compliment those of Kops *et al*., (2004), in which giant multinucleated cells where observed in BubR1-depleted Hela cells following continued exposure to a structurally different tubulin depolymeriser, colcemid. Taken together, these observations imply that BubR1 not only functions as a guardian of the mitotic spindle but also as a key regulator in the execution of cytokinesis.

Further studies investigating the role of BubR1 in cytokinesis are warranted before advances can be made in terms of augmenting MTA-induced cytotoxicity. Specifically, it would be interesting to determine whether phosphorylation of BubR1 is necessary for its role in cytokinesis. Once clarified, this knowledge can be exploited to enhance the apoptotic efficacy of MTAs and other drugs impeded by a prolonged mitotic checkpoint. The Aurora B kinase inhibitor, ZM447439 is a potent inhibitor of BubR1 phosphorylation and spindle checkpoint activation (Ditchfield *et al*., 2003). It may

Molecular Pharmacology Fast Forward. Published on November 8, 2007 as DOI: 10.1124/mol.107.039024
This article has not been copyedited and formatted. The final version may differ from this version.

therefore be of interest to determine any therapeutic benefits in combining ZM447439 with MTAs, including the pyrrolo-1,5-benzoxazepines.

In conclusion, the pyrrolo-1,5-benzoxazepines represent a novel class of MTAs for the effective treatment of carcinomas expressing low endogenous levels of the mitotic spindle checkpoint regulator, BubR1. Moreover, reduction of BubR1 may form a critical link between the spindle checkpoint and induction of apoptosis by tubulin targeting pyrrolo-1,5-benzoxazepines and other MTAs.

References

Acquaviva C, Herzog F, Kraft C and Pines J (2004) The anaphase promoting complex/cyclosome is recruited to centromeres by the spindle assembly checkpoint. *Nat Cell Biol* 6:892-898.

Campiani, G., Fiorini, I., De Filippis, M.P., Ciani, S.M., Garofalo, A., Nacci, V., Giorgi, G., Sega, A., Botta, M., Chiarini, A., Budriesi, R., Bruni, G., Romeo, M.R., Manzoni, C. and Mennini, T. (1996) Cardiovascular characterization of pyrrolo[2,1-d][1,5]benzothiazepine derivatives binding selectively to the peripheral-type benzodiazepine receptor (PBR): from dual PBR affinity and calcium antagonist activity to novel and selective calcium entry blockers. *J Med Chem* 39: 2922-2938.

Chan, G.K., Jablonski, S.A., Sudakin, V., Hittle, J.C. and Yen, T.J. (1999) Human BUBR1 is a mitotic checkpoint kinase that monitors CENP-E functions at kinetochores and binds the cyclosome/APC. *J Cell Biol* 146: 941-954.

Chen RH (2002) BubR1 Is Essential for Kinetochore Localization of Other Spindle Checkpoint Proteins and Its Phosphorylation Requires Mad1. *J Cell Biol* 158: 487-96.

Cleveland, D.W., Mao, Y. and Sullivan, K.F. (2003) Centromeres and kinetochores: from epigenetics to mitotic checkpoint signaling. *Cell* 112: 407-421.

Ditchfield, C., Johnson, V.L., Tighe, A., Ellston, R., Haworth, C., Johnson, T., Mortlock, A., Keen, N. and Taylor, S.S. (2003) Aurora B couples chromosome alignment with anaphase by targeting BubR1, Mad2, and Cenp-E to kinetochores. *J Cell Biol* 161: 267-280.

Doncic, A., Ben-Jacob, E. and Barkai, N. (2005) Evaluating putative mechanisms of the mitotic spindle checkpoint. *Proc Natl Acad Sci U S A* 102: 6332-6337.

Garcia, A.A., Leichman, C.G., Lenz, H.J., Baranda, J., Lujan, R., Casagrande, Y. and Leichman, L. (2001) Phase II trial of outpatient schedule of paclitaxel in patients with previously untreated metastatic, measurable adenocarcinoma of the stomach. *Jpn J Clin Oncol* 31: 275-278.

Grabsch, H., Takeno, S., Parsons, W.J., Pomjanski, N., Boecking, A., Gabbert, H.E. and Mueller, W. (2003) Overexpression of the mitotic checkpoint genes BUB1, BUBR1, and BUB3 in gastric cancer-association with tumour cell proliferation. *J Pathol* 200: 16-22.

Greene, L.M., Fleeton, M., Mulligan, J., Gowda, C., Sheahan, B.J., Atkins, G.J., Campiani, G., Nacci, V., Lawler, M., Williams, D.C. and Zisterer, D.M. (2005) The pyrrolo-1,5-benzoxazepine, PBOX-6, inhibits the growth of breast cancer cells in vitro independent of estrogen receptor status and inhibits breast tumour growth *in vivo*. *Oncol Rep* 14: 1357-1363.

Holt SV, Vergnolle MA, Hussein D, Wozniak MJ, Allan VJ, Taylor SS (2005) Silencing Cenp-F weakens centromeric cohesion, prevents chromosome alignment and activates the spindle checkpoint. *J Cell Sci* 118: 4889-4900.

Jordan, M.A. (2002) Mechanism of action of antitumor drugs that interact with microtubules and tubulin. *Curr Med Chem Anticancer Agents* 2: 1-17.

Johnson VL, Scott M I, Holt S V, Hussein D and Taylor S S (2004) Bub1 Is Required for Kinetochore Localization of BubR1, Cenp-E, Cenp-F and Mad2, and Chromosome

Congression. *J Cell Sci* 117: 1577-1589.

Kim, M., Murphy, K., Liu, F., Parker, S.E., Dowling, M.L., Baff, W. and Kao, G.D. (2005) Caspase-mediated specific cleavage of BubR1 is a determinant of mitotic progression. *Mol Cell Biol* 25: 9232-9248.

Kops, G.J., Foltz, D.R. and Cleveland, D.W. (2004) Lethality to human cancer cells through massive chromosome loss by inhibition of the mitotic checkpoint. *Proc Natl Acad Sci U S A* 101: 8699-8704.

Lee, E.A., Keutmann, M.K., Dowling, M.L., Harris, E., Chan, G. and Kao, G.D. (2004) Inactivation of the mitotic checkpoint as a determinant of the efficacy of microtubule-targeted drugs in killing human cancer cells. *Mol Cancer Ther* 3: 661-669.

Li, W., Lan, Z., Wu, H., Wu, S., Meadows, J., Chen, J., Zhu, V. and Dai, W. (1999) BUBR1 phosphorylation is regulated during mitotic checkpoint activation. *Cell Growth Differ* 10: 769-775.

Logarinho, E., Bousbaa, H., Dias, J.M., Lopes, C., Amorim, I., Antunes-Martins, A. and Sunkel, C.E. (2004) Different spindle checkpoint proteins monitor microtubule attachment and tension at kinetochores in Drosophila cells. *J Cell Sci* 117: 1757-1771.

Meraldi P, Draviam V M and Sorger P K (2004) Timing and Checkpoints in the Regulation of Mitotic Progression. *Dev Cell* 7: 45-60.

Mc Gee, M.M., Campiani, G., Ramunno, A., Fattorusso, C., Nacci, V., Lawler, M., Williams, D.C. and Zisterer, D.M. (2001) Pyrrolo-1,5-benzoxazepines induce apoptosis

in chronic myelogenous leukemia (CML) cells by bypassing the apoptotic suppressor bcr-abl. *J Pharmacol Exp Ther* 296: 31-40.

Mc Gee MM, Hyland E, Campiani G, Ramunno A, Nacci V and Zisterer D M (2002a) Caspase-3 Is Not Essential for DNA Fragmentation in MCF-7 Cells During Apoptosis Induced by the Pyrrolo-1,5-Benzoxazepine, PBOX-6. *FEBS Lett* 515: 66-70.

Mc Gee, M.M., Campiani, G., Ramunno, A., Nacci, V., Lawler, M., Williams, D.C. and Zisterer, D.M. (2002b) Activation of the c-Jun N-terminal kinase (JNK) signaling pathway is essential during PBOX-6-induced apoptosis in chronic myelogenous leukemia (CML) cells. *J Biol Chem* 277: 18383-18389.

Mc Gee, M.M., Greene, L.M., Ledwidge, S., Campiani, G., Nacci, V., Lawler, M., Williams, D.C. and Zisterer, D.M. (2004) Selective induction of apoptosis by the pyrrolo-1,5-benzoxazepine 7-[[dimethylcarbamoyl]oxy]-6-(2-naphthyl) pyrrol-[2,1-d] (1,5)-benzoxazepine (PBOX-6) in Leukemia cells occurs via the c-Jun NH2-terminal kinase-dependent phosphorylation and inactivation of Bcl-2 and Bcl-XL. *J Pharmacol Exp Ther* 310: 1084-1095.

Mollinedo, F. and Gajate, C. (2003) Microtubules, microtubule-interfering agents and apoptosis. *Apoptosis* 8: 413-450.

Mulligan, J.M., Greene, L.M., Cloonan, S., Mc Gee, M.M., Onnis, V., Campiani, G., Fattorusso, C., Lawler, M.P., Williams, C. and Zisterer, D.M. (2006) Identification of tubulin as the molecular target of pro-apoptotic pyrrolo-1,5-benzoxazepines. *Mol Pharmacol* 70: 60-70.

Ofir R, Seidman R, Rabinski T, Krup M, Yavelsky V, Weinstein Y and Wolfson M (2002) Taxol-Induced Apoptosis in Human SKOV3 Ovarian and MCF7 Breast Carcinoma Cells Is Caspase-3 and Caspase-9 Independent. *Cell Death Differ* 9: 636-642.

Peters, J.M. (2002) The anaphase-promoting complex: proteolysis in mitosis and beyond. *Mol Cell* 9: 931-943.

Shin, H.J., Baek, K.H., Jeon, A.H., Park, M.T., Lee, S.J., Kang, C.M., Lee, H.S., Yoo, S.H., Chung, D.H., Sung, Y.C., McKeon, F. and Lee, C.W. (2003) Dual roles of human BubR1, a mitotic checkpoint kinase, in the monitoring of chromosomal instability. *Cancer Cell* 4: 483-497.

Sudo, T., Nitta, M., Saya, H. and Ueno, N.T. (2004) Dependence of paclitaxel sensitivity on a functional spindle assembly checkpoint. *Cancer Res* 64: 2502-2508.

Tang, C., Willingham, M.C., Reed, J.C., Miyashita, T., Ray, S., Ponnathpur, V., Huang, Y., Mahoney, M.E., Bullock, G. and Bhalla, K. (1994) High levels of p26BCL-2 oncoprotein retard taxol-induced apoptosis in human pre-B leukemia cells. *Leukemia* 8: 1960-1969.

Taylor SS, Hussein D, Wang Y, Elderkin S and Morrow C J (2001) Kinetochore Localisation and Phosphorylation of the Mitotic Checkpoint Components Bub1 and BubR1 Are Differentially Regulated by Spindle Events in Human Cells. *J Cell Sci* 114: 4385-4395.

Yu, D., Jing, T., Liu, B., Yao, J., Tan, M., McDonnell, T.J. and Hung, M.C. (1998)

Overexpression of ErbB2 blocks Taxol-induced apoptosis by upregulation of p21Cip1, which inhibits p34Cdc2 kinase. *Mol Cell* 2: 581-591.

Zisterer, D.M., Campiani, G., Nacci, V. and Williams, D.C. (2000) Pyrrolo-1,5-benzoxazepines induce apoptosis in HL-60, Jurkat, and Hut-78 cells: a new class of apoptotic agents. *J Pharmacol Exp Ther* 293: 48-59.

Molecular Pharmacology Fast Forward. Published on November 8, 2007 as DOI: 10.1124/mol.107.039024
This article has not been copyedited and formatted. The final version may differ from this version.

Footnotes

We would like to thank Science Foundation Ireland for funding the project. Sincere thanks to Dr. Orla Hanrahan (School of Biochemistry and Immunology, TCD) for her technical assistance on the confocal microscope and to Dr. Stephen Taylor (School of Biological Sciences, University of Manchester) for his helpful advice on achieving optimal tubulin and chromosome staining. Reprint requests: Lisa Greene, School of Biochemistry and Immunology, Trinity College, Dublin 2, Ireland. E-mail: greeneli@tcd.ie. We thank the anonymous reviewers of the manuscript for their helpful suggestions.

Molecular Pharmacology Fast Forward. Published on November 8, 2007 as DOI: 10.1124/mol.107.039024
This article has not been copyedited and formatted. The final version may differ from this version.

Figure legends

Figure 1: PBOX-15 is a more potent anti-mitotic analogue of PBOX-6. Logarithmically growing K562 cells were exposed to vehicle [0.2% ethanol (v/v)], PBOX-6 or -15 [0.1-10 μM] for 16 h (A) or PBOX-6 [10 μM] or PBOX-15 [1 μM] for 1-72 h (B, C). Cells were then fixed, stained with PI and analysed by flow cytometry. Cell cycle analysis was performed on histograms of gated counts per DNA area (FL2-A). The number of cells with <2N (pre-G1), 2N (G_0G_1), 4N (G_2M), >4N (polyploid cells) DNA content was determined using the Cell Quest software. The pre-G1 peak is indicative of apoptosis. Values represent the mean ± SEM for at least three separate experiments. The absence of error bars indicates that the error was smaller than the size of the symbol.

Figure 2: BubR1 phosphorylation is associated with PBOX-induced G_2M cell cycle arrest in human CML K562 cells. A, K562 cells in the log phase of growth were exposed to vehicle (V) [0.2% ethanol (v/v)], PBOX-6 or -15 [0.1-10 μM] for 16 h. B, K562 cells were exposed to vehicle (V) [0.1% DMSO] or nocodazole [0.5 μM] for 16 h. C, K562 cells were exposed to vehicle (V) [0.2% ethanol (v/v)], PBOX-15 (P) [1 μM] or nocodazole (N) [0.5 μM] for 1-48 h. Whole cell lysates were resolved by SDS-PAGE and probed with anti-BubR1 mouse mAb. Results are representative of three separate experiments. Blots were probed with anti-actin mAb as a loading control. BubR1-P, hyperphosphorylated form. BubR1, unphosphorylated form.

Molecular Pharmacology Fast Forward. Published on November 8, 2007 as DOI: 10.1124/mol.107.039024
This article has not been copyedited and formatted. The final version may differ from this version.

Figure 3: Endogenous levels of mitotic spindle checkpoint proteins, BubR1 and Bub3, predict the type of cellular response to MTAs. A, equal amounts (50 µg) of whole cell lysates were analysed by western blotting using anti-BubR1 and anti-Bub3 mAbs. Blots were probed with actin as a loading control. Results are representative of at least three separate experiments. B, sub-confluent cells were either treated with MTAs (P6, PBOX-6 [10 µM]; P15, PBOX-15 [1 µM]; or Noc, Nocodazole [0.5 µM]) or relevant vehicle (E, [0.2% ethanol (v/v)]; D, [0.1% DMSO (v/v)]) for the time indicated. Cells were then fixed, stained with PI and analysed by flow cytometry. Percentage apoptosis was determined by quantification of the pre-G1 peak. The percentage of cells in the G_2M phase of the cell cycle is also indicated. Values represent the means for at least three separate experiments ± S.E.M.

Figure 4: Phosphorylation of BubR1 correlates with G_2M cell cycle arrest and down-regulation of BubR1 correlates with apoptosis in human cancer cells treated with MTAs. Whole-cell extracts were prepared from each cell line following treatment with MTAs (P6, PBOX-6 [10 µM]; P15, PBOX-15 [1 µM]; N, Nocodazole [0.5 µM]) or relevant vehicle (E, [0.2% ethanol (v/v)]; D, [0.1% DMSO (v/v)]) for the time indicated. Lysates were resolved by SDS-PAGE and probed with anti-PARP (A) and anti-BubR1 mAbs (B). Blots were probed with anti-actin monoclonal antibody as a loading control. The mean percentage of cells in the pre-G1 peak (apoptotic) and G_2M phase of the cell cycle are also indicated. Results shown are representative of three independent experiments.

Molecular Pharmacology Fast Forward. Published on November 8, 2007 as DOI: 10.1124/mol.107.039024
This article has not been copyedited and formatted. The final version may differ from this version.

Figure 5: Effects of PBOX-15 on the microtubule network and localization of BubR1 in prometaphase and metaphase cells. Phase contrast and confocal fluorescent images of normal (control) and PBOX-15 [1 μM] treated Hela cells. Projections of multiple confocal sections along z-axis show Hela cells stained with DM1A (anti-tubulin, green), SBR1.1 (anti-BubR1, red) and Hoechst (blue). Scale bars represent 10 μM.

Figure 6: siRNA repression of BubR1 leads to increased polyploidy following mitotic spindle disruption in human cervical carcinoma-derived cells. A, Hela cells were left untreated or exposed to siRNA duplexes for the time indicated after which the medium was replaced with DMEM medium containing 20% FCS. Cells were harvested at 48 h post-transfection. In B, cells were exposed to the indicated siRNA duplexes for 4 h. Cells were harvested at 24-72 h post-transfection. Scrambled siRNA concentration is 100 nM (A) and 50 nM (B). A and B, equal amounts of whole cell lysates were separated by SDS-PAGE and probed with anti-BubR1 mAb. Blots were probed with anti-actin mAb as a loading control. Results shown are representative of three separate experiments. C, Hela cells were transfected with control (scrambled) or BubR1 siRNA duplexes at a final concentration of 50 nM for 4h, cultured in DMEM with 20% FCS for a further 20 h, and subsequently treated with ethanol vehicle [0.2% (v/v)], DMSO [0.1% (v/v)], PBOX-15 [1 μM] or nocodazole [0.5 μM] and harvested after 48 h. Cell cycle analysis was performed on histograms of gated counts per DNA area (FL2-A). Relative percentage of cells with <2N (Pre-G1; apoptotic), 2N (G_0G_1), 4N (G_2M) or >4N (polyploid) DNA content were derived from the analysis of DNA histograms using the Cell Quest software. Results are representative of three separate experiments. Values represent the mean ±

Molecular Pharmacology Fast Forward. Published on November 8, 2007 as DOI: 10.1124/mol.107.039024
This article has not been copyedited and formatted. The final version may differ from this version.

SEM for at least three separate experiments. (**, P < 0.01, ***, P <0.001; paired Student's *t* test).

Figure 7: Effects of BubR1-depletion of PBOX-15-induced cell death. Hela cells were transfected with BubR1 or scrambled siRNA duplexes as described in materials and methods. After 24 h, cells were then treated with control vehicle [0.2% ethanol (v/v)] or PBOX-15 [1 μM] for time indicated. A, representative overlays of log DNA histograms demonstrating the effect of PBOX-15 (open histograms) on Hela cells transfected with BubR1 or scrambled siRNA complexes after 2 (2 D) and 4 days (4 D). Vehicle treated cells are represented with shaded histograms. DNA content of the cells are indicated (<2N{Pre-G1; apoptotic}, 2N (G_0G_1), 4N (G_2M) or >4N {polyploidy}) below histograms and were derived using the Cell Quest software. B, western blotting showing PARP cleavage and Bub3 protein levels in siRNA transfected cells treated with ethanol vehicle (E), DMSO vehicle (D), PBOX-15 (P15) or nocodazole (N) for 2 days. Knockdown of BubR1 was confirmed by probing blots with anti-BubR1. Blots were probed with anti-actin as a loading control. C, siRNA transfected cells were treated with either ethanol (control) or PBOX-15 for 4 days. Cells were then fixed and stained with Hoechst (blue) and anti-tubulin antibodies (green). Bar is equal to 40 μM. All results shown are representative of at least three separate experiments.

Figure 8: Targeted inhibition of BubR1 increases polyploidy in human MDA-MB-231 breast carcinoma-derived cells following a prolonged mitotic disruption. Cells were transfected with 50 nM BubR1 or scrambled siRNA duplexes for 4 h and cultured

Molecular Pharmacology Fast Forward. Published on November 8, 2007 as DOI: 10.1124/mol.107.039024
This article has not been copyedited and formatted. The final version may differ from this version.

in DMEM supplemented with 20% FCS thereafter. A, western blot showing repression of BubR1 at 24 and 48 h post-transfection. Actin was used as a loading control. B, at 24 h post-transfection cells were treated with relevant vehicle, PBOX-15 [1 μM] or nocodazole [0.5 μM] for 48 h. Cells were then fixed, stained with PI and analysed by flow cytometry. Cell cycle analysis was performed on histograms of gated counts per DNA area (FL2-A). Relative percentage of cells with <2N (Pre-G1; apoptotic), 2N (G_0G_1), 4N (G_2M), <4N (polyploid) DNA content were derived from the analysis of DNA histograms using the Cell Quest software. Results are representative of three separate experiments. Values represent the mean ± SEM for at least three separate experiments (*, $P < 0.05$; paired Student's *t* test).

A

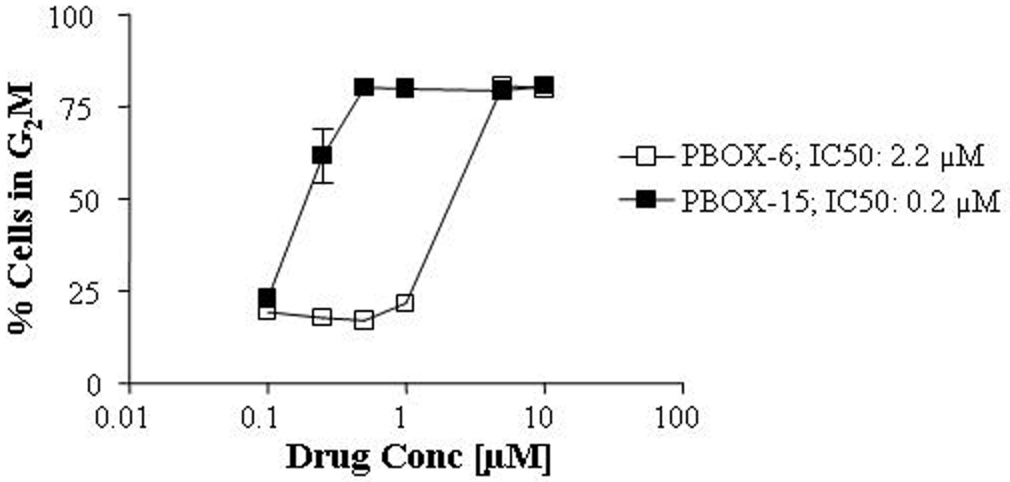
100
75
50
25
0
% Cells in G2M
0.01
0.1
1
10
100
Drug Conc [µM]
PBOX-6; IC50: 2.2 µM
PBOX-15; IC50: 0.2 µM

B

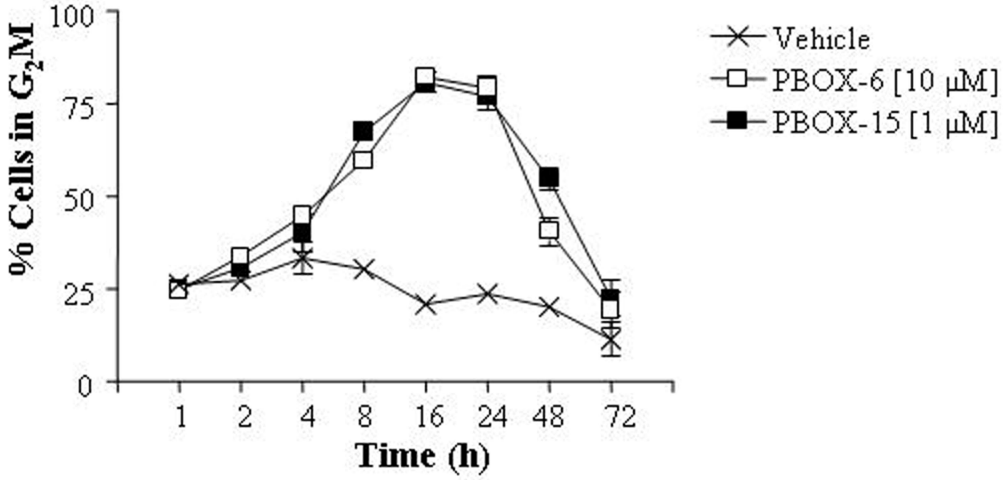
100
75
50
25
0
% Cells in G2M
1
2
4
8
16
24
48
72
Time (h)
Vehicle
PBOX-6 [10 µM]
PBOX-15 [1 µM]

C

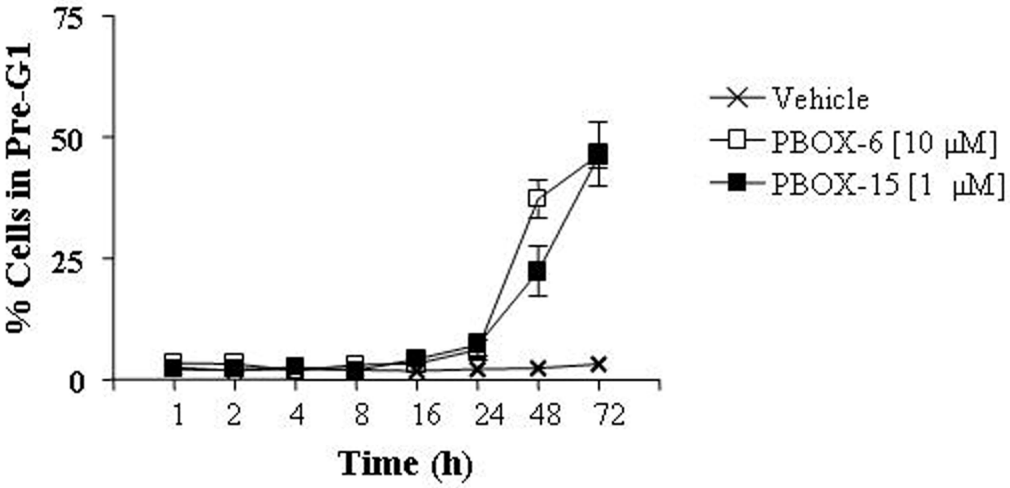
75
50
25
0
% Cells in Pre-G1
1
2
4
8
16
24
48
72
Time (h)
Vehicle
PBOX-6 [10 µM]
PBOX-15 [1 µM]

Figure 1

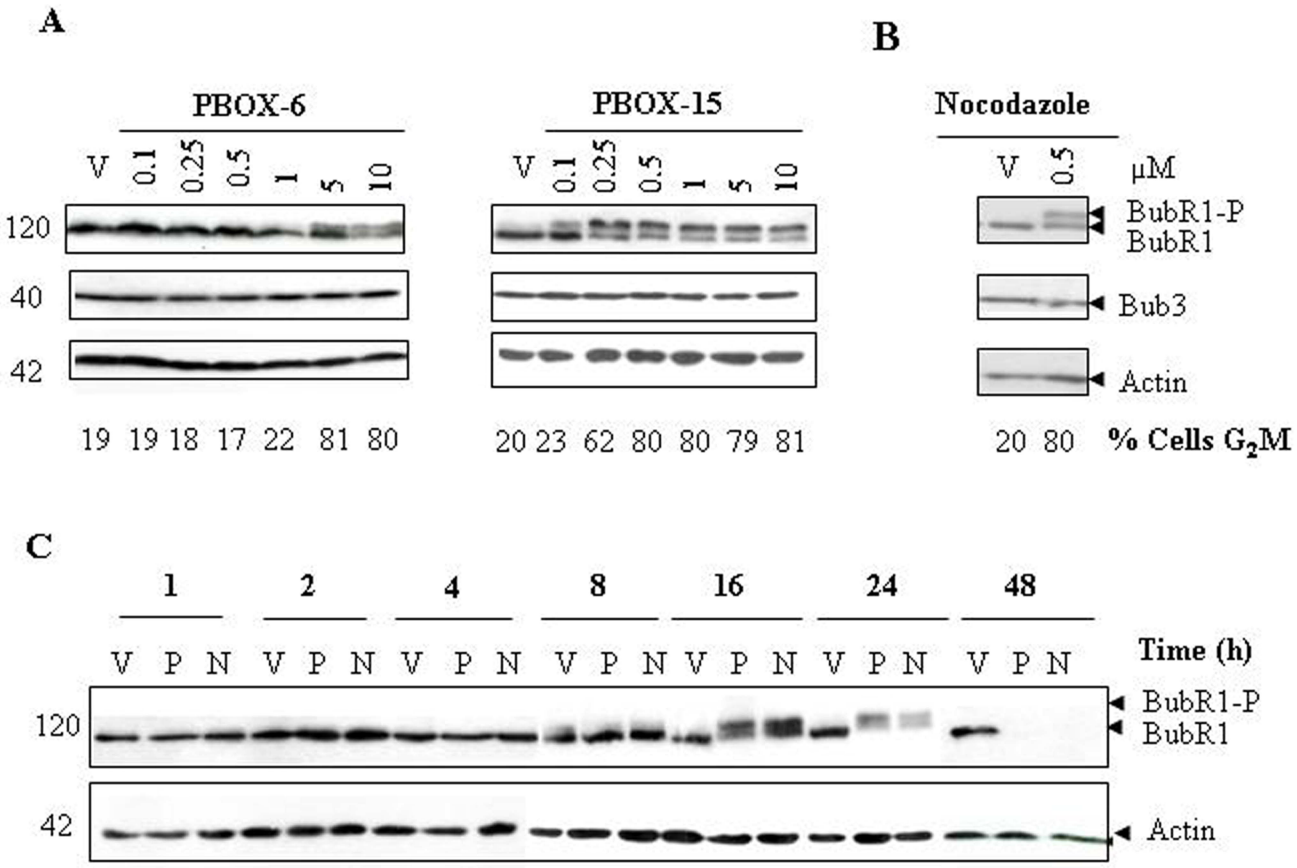
A
PBOX-6
V 0.1 0.25 0.5 1 5 10
120
40
42
19 19 18 17 22 81 80
PBOX-15
V 0.1 0.25 0.5 1 5 10
20 23 62 80 80 79 81
B
Nocodazole
V 0.5 µM
BubR1-P
BubR1
Bub3
Actin
20 80 % Cells G2M
C
1 2 4 8 16 24 48
V P N V P N V P N V P N V P N V P N V P N
Time (h)
120
42
BubR1-P
BubR1
Actin

Figure 2

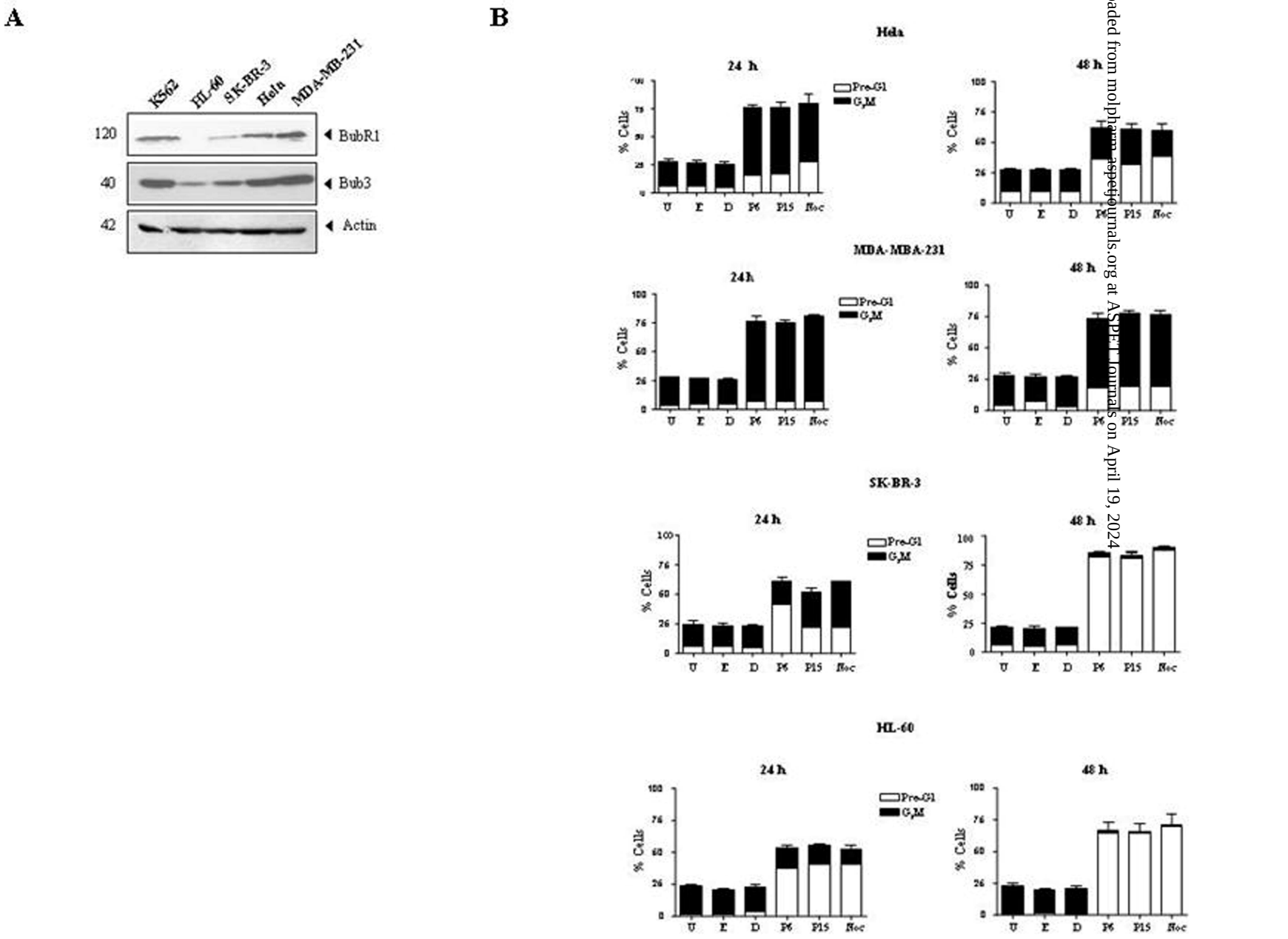

Figure 3

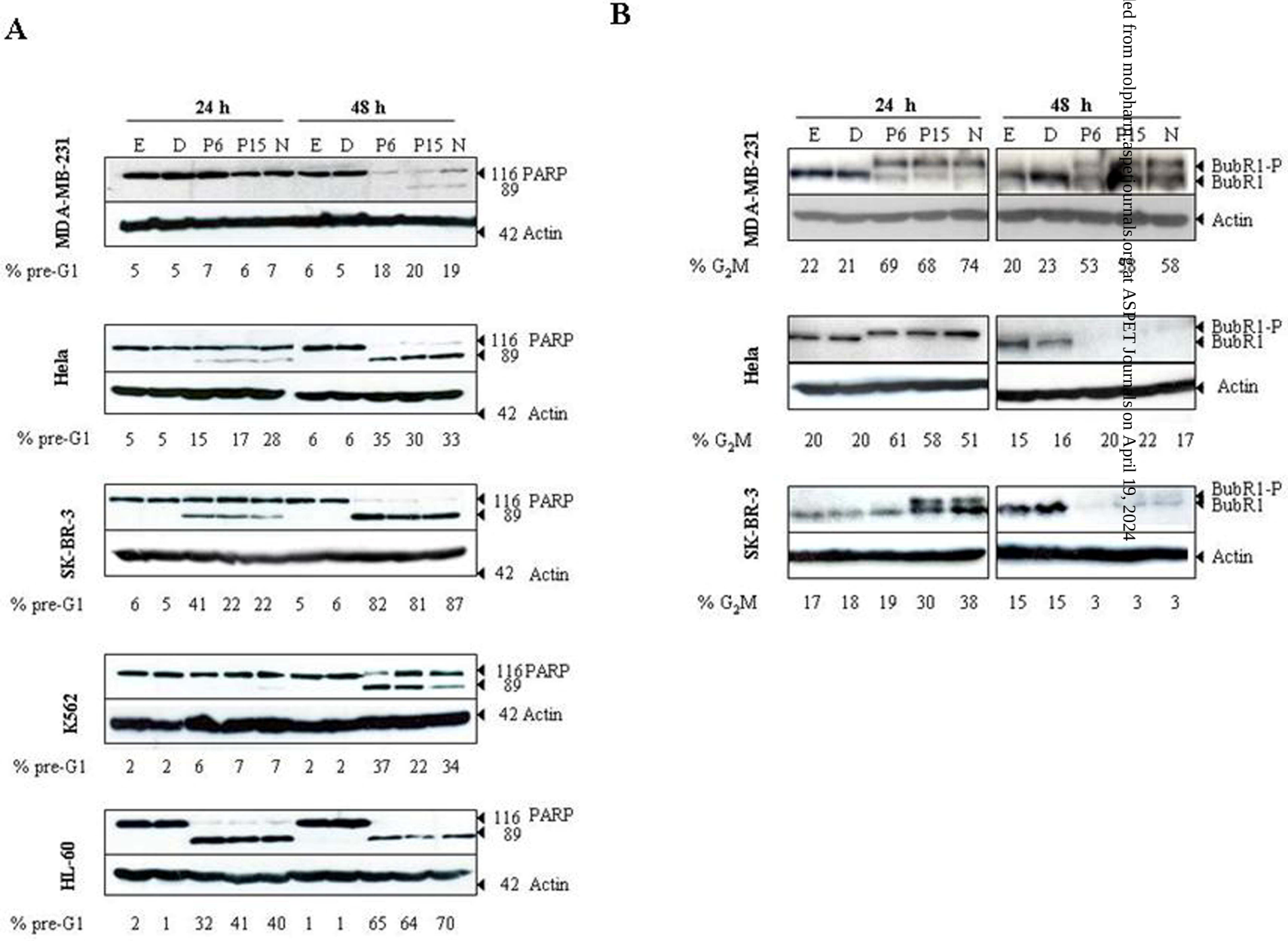

Figure 4

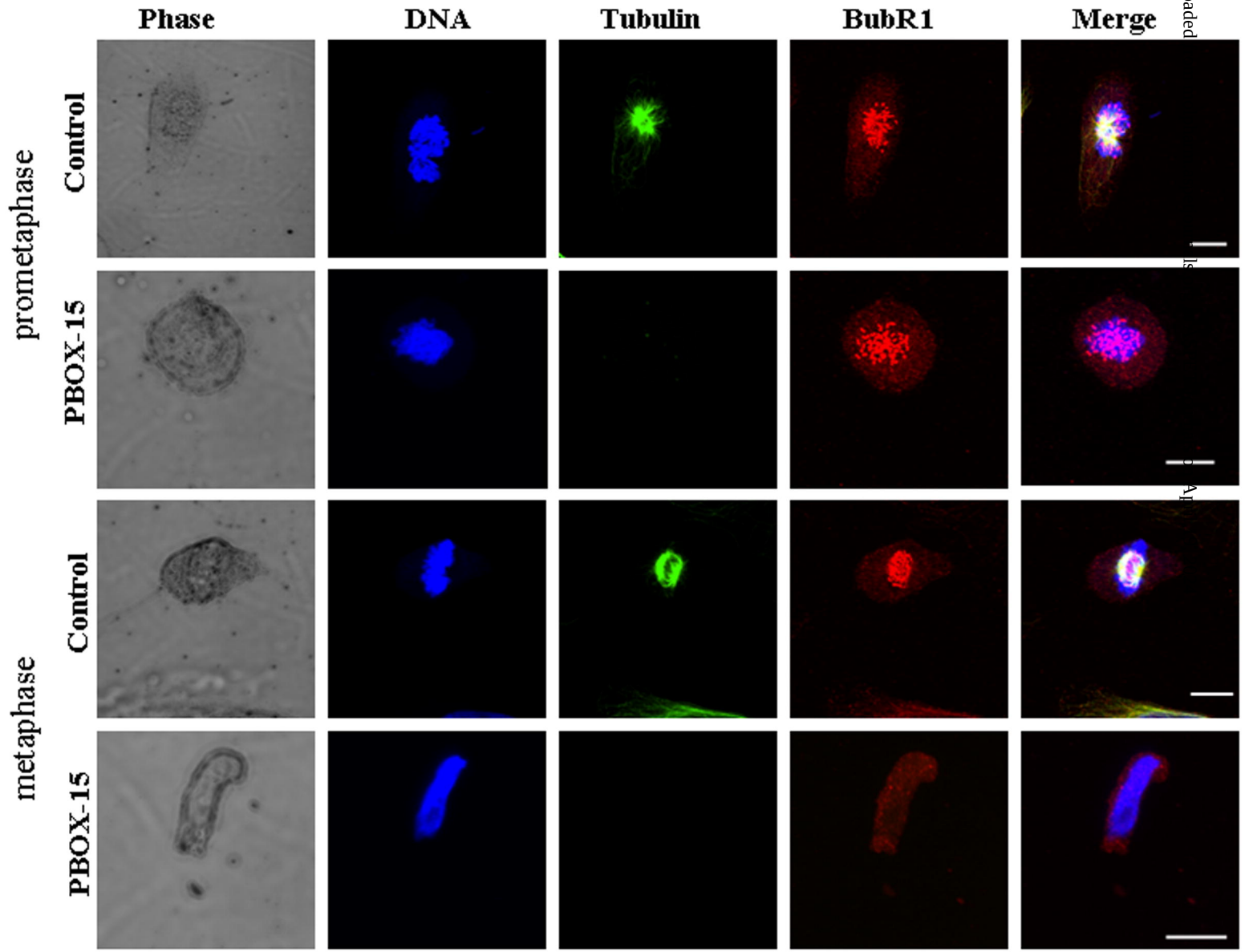
Phase
DNA
Tubulin
BubR1
Merge
prometaphase
metaphase
Control
PBOX-15
Control
PBOX-15

Figure 5

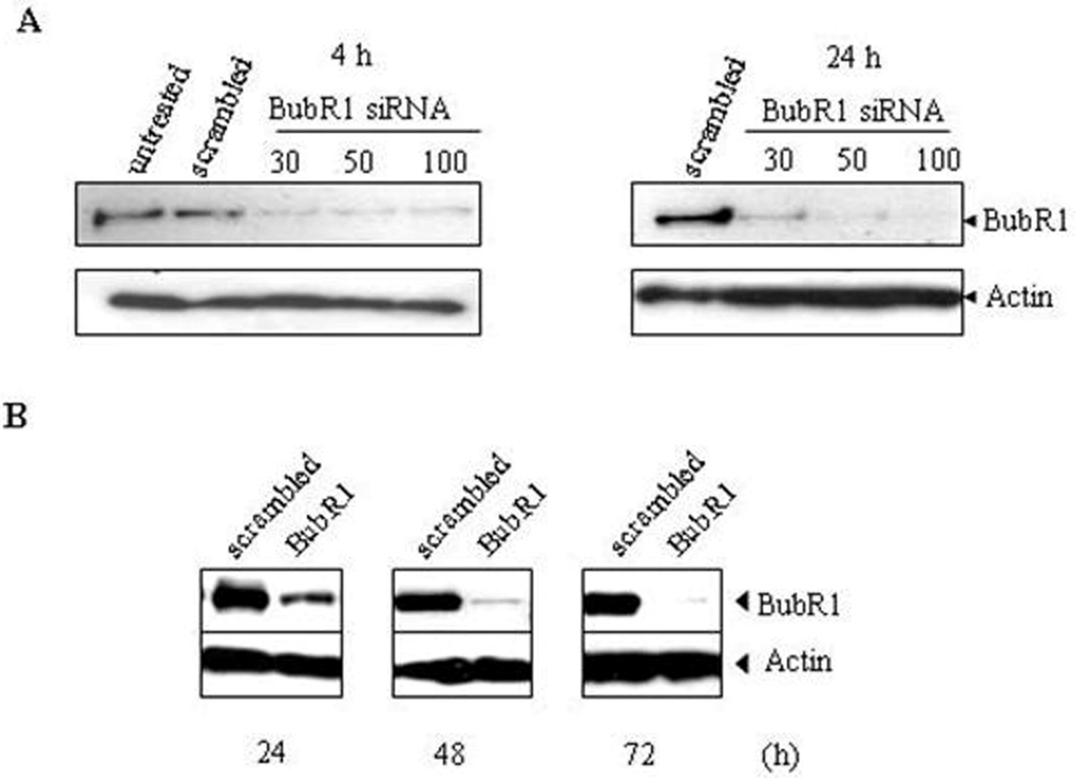
A
4 h
untreated
scrambled
BubR1 siRNA
30
50
100
24 h
scrambled
BubR1 siRNA
30
50
100
BubR1
Actin
B
scrambled
BubR1
scrambled
BubR1
scrambled
BubR1
BubR1
Actin
24
48
72
(h)

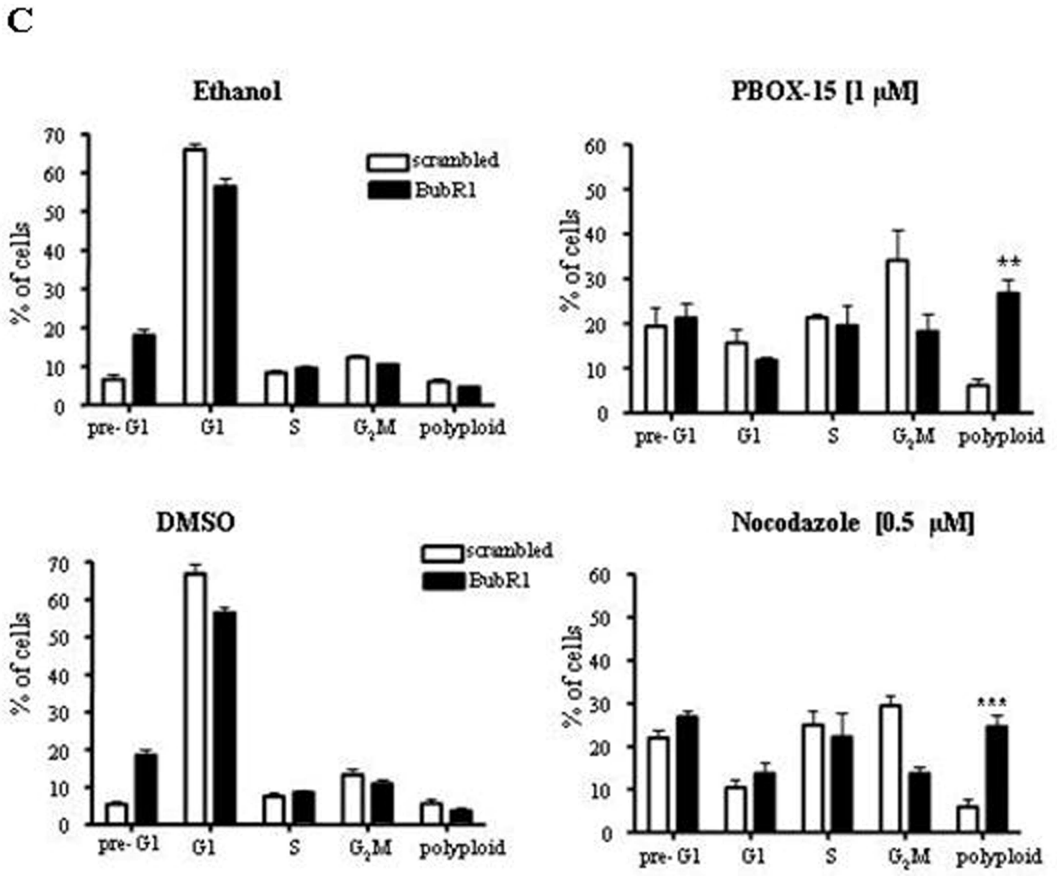
C
Ethanol
scrambled
BubR1
% of cells
pre-G1
G1
S
G2M
polyploid
PBOX-15 [1 μM]
**
DMSO
Nocodazole [0.5 μM]
***

Figure 6

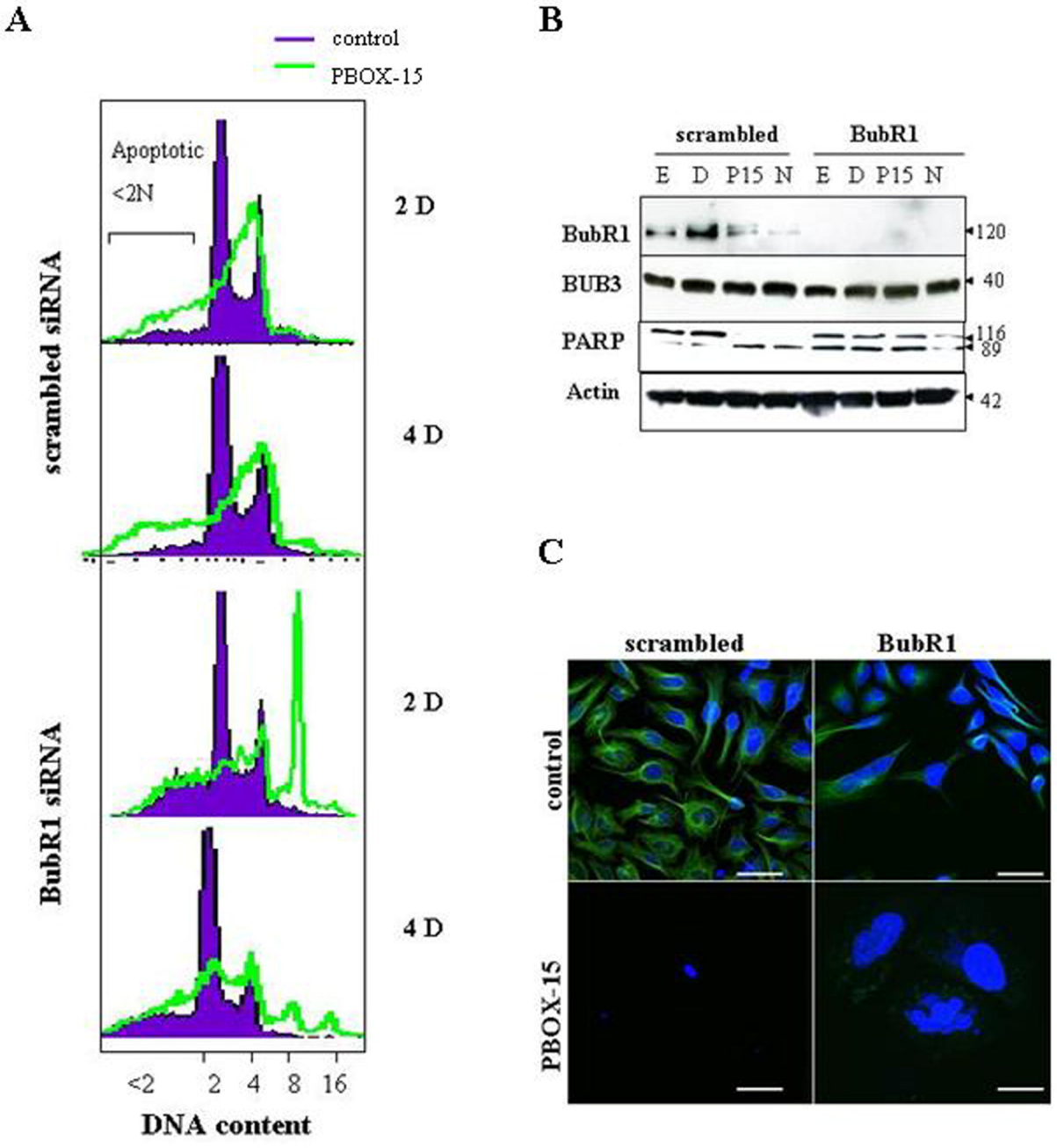
A
control
PBOX-15
Apoptotic
<2N
2 D
4 D
scrambled siRNA
BubR1 siRNA
2 D
4 D
<2
2
4
8
16
DNA content
B
scrambled
BubR1
E D P15 N E D P15 N
BubR1
BUB3
PARP
Actin
120
40
116
89
42
C
scrambled
BubR1
control
PBOX-15

Figure 7

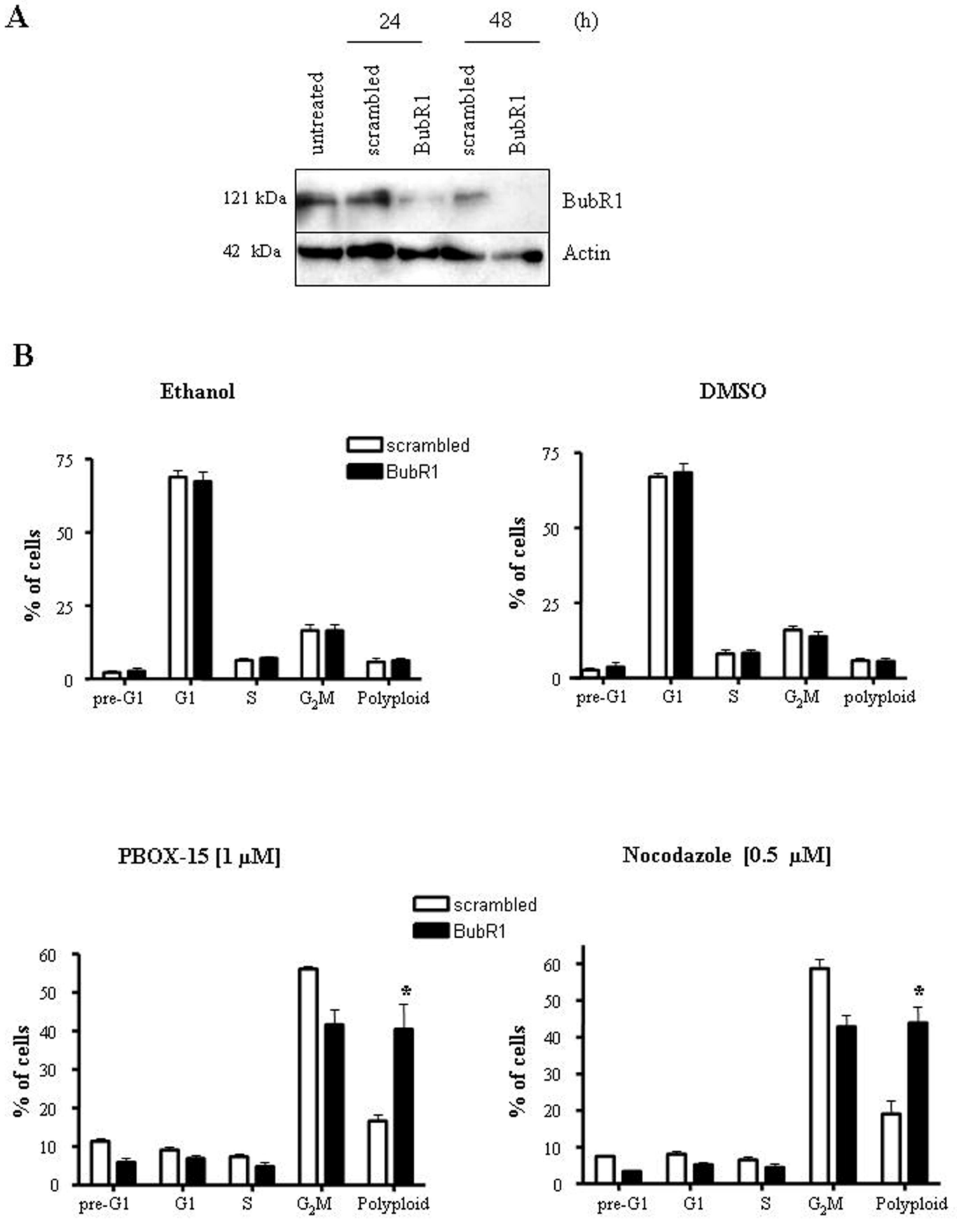
A
24
48
(h)
untreated
scrambled
BubR1
scrambled
BubR1
121 kDa
BubR1
42 kDa
Actin
B
Ethanol
DMSO
scrambled
BubR1
% of cells
75
50
25
0
pre-G1
G1
S
G2M
Polyploid
polyploid
PBOX-15 [1 μM]
Nocodazole [0.5 μM]
60
50
40
30
20
10
*

Figure 8